Investigation of High-Spin States in Er^{166}†

J. E. Cline and C. W. Reich
National Reactor Testing Station, Phillips Petroleum Company, Idaho Falls, Idaho
(Received 10 October 1962)

The decay of the long-lived isomer of Ho^{166} has been studied using gamma-ray scintillation spectrometers and silicon-diode detectors. The results of gamma-gamma coincidence experiments, together with least-squares analysis of the gamma-ray singles spectra, establish the presence of twenty-seven gamma-ray transitions in the decay of this isomer. The conversion-electron spectra provide relative intensities for several of the weak transitions and provided an upper limit for the endpoint energy of the main beta transition from Ho^{166}. The data are consistent with the existence of levels whose energies (in keV) and assignments are 80 (2+), 265 (4+), 545 (6+), 787 (2+), 861 (3+), 910 (8+), 957 (4+), 1074 (5+), 1220 (6+), 1374 (7+), 1680 (5−), 1785 (6−), and 1840 (6−). The data indicate that the energy of the most intense beta transition from the long-lived Ho^{166} state must lie between ≈ 55 and ≈ 65 keV. Several possible nucleon configurations for the negative-parity states in Er^{166} observed in the decay of this activity are presented and discussed. A description of the observed positive-parity states in terms of an asymmetric-rotator model is given. The agreement between the energies and relative transition probabilities calculated using this model and those observed experimentally is excellent. Formulas for reduced transition probabilities for gamma-ray transitions between states having spins of 6, 7, and 8 are presented.

I. INTRODUCTION

THE level structure of highly deformed even-even nuclei exhibits certain features which have been interpreted as evidence for collective rotations. In particular, two apparent sequences of positive-parity states are observed at excitation energies below ~ 1 MeV. In each of these sequences a spin-2 state is observed. Two models of the nucleus are currently used to describe these nuclear states. The unified model, introduced by Bohr and Mottelson,[1] interprets the higher-energy 2+ state as a vibrational excitation of the ground state. Remaining levels in the second sequence are then described as rotational excitations of this vibrational state. In the asymmetric-rotator model, as developed by Davydov,[2,3] however, this state as well as the other states of the sequence are described as rotational excitations of the ground-state configuration.

Since very little experimental evidence exists concerning the properties of high-spin states in these nuclei, the applications of these two nuclear models has been confined primarily to states of relatively low spin. It should be of considerable interest, therefore, to investigate the decay characteristics of nuclides which excite the higher spin states of even-even highly deformed daughter nuclei. The decay of the long-lived Ho^{166} isomer excites such levels and an investigation of its decay scheme was therefore undertaken at this laboratory.

Levels in Er^{166} are fed through the β^- decay of two states[4] in Ho^{166} and through electron capture[5–7] in Tm^{166}. The decay of 27-h Ho^{166} [8–15] populates levels in Er^{166} which have spins of 2 or less. Electron capture in Tm^{166}, on the other hand, populates primarily those levels having spins of 4 or less. In the decay of the long-lived Ho^{166} isomer, states of presumably higher spin ($5 \rightarrow 8$), as well as the lower lying low-spin levels, are observed. The decay of the longer lived Ho^{166} activity has received relatively little study and details of the decay scheme have remained unclear. Several studies of the gamma rays emitted in the decay have been made using scintillation spectrometers.[16–19] Investigations of the electrons emitted in the decay have also been made[18–20] using magnetic spectrometers. The results of these investigations have neither led to a

† Work performed under the auspices of the U. S. Atomic Energy Commission.

[1] R. K. Sheline, Rev. Mod. Phys. **32**, 1 (1960).
[2] A. S. Davydov and G. F. Filippov, Nucl. Phys. **8**, 237 (1958).
[3] C. A. Mallmann, Nucl. Phys. **24**, 535 (1961).
[4] F. D. S. Butement, Proc. Phys. Soc. (London) **65**, 254 (1952).
[5] K. P. Jacob, J. W. Mihelich, B. Harmatz, and T. H. Handley, Phys. Rev. **117**, 1102 (1960).
[6] K. Gromov, B. Dzhelepov, and B. Preobrazhenskii, Izv. Akad. Nauk. SSSR (Ser. Fiz.) **21**, 918 (1957).
[7] B. Harmatz, T. H. Handley, and J. W. Mihelich, Phys. Rev. **123**, 1758 (1960).
[8] A. W. Sunyar, Phys. Rev. **93**, 1345 (1954).
[9] J. M. Cork, M. K. Brice, R. G. Helmer, and R. M. Woods, Jr., Phys. Rev. **110**, 526 (1958).
[10] J. S. Fraser and J. C. Milton, Phys. Rev. **98**, 1173A (1955).
[11] R. L. Graham, M. L. Wolfson, and M. A. Clark, Phys. Rev. **98**, 1173A (1955).
[12] E. Berlovic, Izv. Akad. Nauk. SSSR (Ser. Fiz.) **20**, 1438 (1956).
[13] I. Marklund, R. Van Nooijen, and Z. Grabowski, Nucl. Phys. **15**, 533 (1960).
[14] P. G. Hansen, K. Wilski, D. J. Horen, and Lung-Wen Chiao, Nucl. Phys. **24**, 519 (1961).
[15] J. E. Cline, E. C. Yates, and E. H. Turk, Nucl. Phys. **30**, 154 (1962).
[16] J. C. Milton, J. S. Fraser, and G. M. Milton, Phys. Rev. **98**, 1173A (1955).
[17] M. A. Grace, R. T. Taylor, and P. B. Treacy, Phil. Mag. **3**, 90 (1958).
[18] P. Boskma and H. DeWaard, Nucl. Phys. **12**, 533 (1959).
[19] S. Jha, H. G. Devare, M. Narayana Rao, and G. C. Pramila, Nucl. Sci. Abstr. **15**, 279 (1961).
[20] J. S. Geiger, R. L. Graham, and G. T. Ewan, Nucl. Phys. **30**, 409 (1962).

unique decay scheme for this nuclide nor resulted in the determination of a consistent disintegration energy[18–20] for the decay.

We have investigated the radiations emitted in the decay of the long-lived isomer of Ho^{166} using NaI(Tl) scintillation spectrometers and silicon-diode detectors. The proposed decay scheme contains 27 gamma-ray transitions which have been observed in this work and provides a consistent and apparently unique level structure for Er^{166}. The energies of the levels in Er^{166} and experimental relative transition probabilities between these levels have been compared to those of an asymmetric-rotator model of the nucleus and good agreement is obtained. An estimate is made of the disintegration energy.

II. EXPERIMENTAL TECHNIQUES AND DATA

A. Source Preparation

Sources of the long-lived Ho^{166} activity were prepared by irradiation of commercial grade Ho_2O_3 in a high-flux facility of the Materials Testing Reactor ($\approx 4\times 10^{14}$ n/cm^2 sec) for periods of 3 months. After allowing the 27-h activity to decay out, the irradiated samples were purified through the use of a Dowex $50=X12$ cation resin column using $0.4M$ alpha-hydroxyisobutyric acid, pH 3.2, as the eluting agent. Three successive column purifications were made on each sample. Tm^{170}, Er^{169}, and Tb^{160}, present as contaminants, were removed in the first purification. In the two subsequent purifications, no rare-earth activities other than Ho^{166} were observed even though their presence in amounts corresponding to disintegration rates of 0.01% of that of the Ho activity would have been detected. Chemical separations obtained previously with this column on mixtures of rare-earth activities have shown no evidence of elemental contamination in samples taken from the maxima of the elution curves.

Sources 5 mm in diameter were prepared for the gamma-ray studies by evaporation of a weak nitric acid solution of purified Ho on 10 mg/cm² plastic films. Sources 6 mm in diameter were prepared for electron studies by evaporation of the acid solution onto 0.25-mil rubber-hydrochloride films coated on both sides with ≈ 20 $\mu g/cm^2$ of gold.

B. Gamma-Ray Measurements

The gamma radiation emitted in the decay of the Ho^{166} isomer was observed with 3-in.-diameter×3-in.-cylindrical NaI(Tl) detectors. In order to study the effects of coincidence summing in the detector, spectra were taken at several source-detector distances from 10 to 40 cm along the axis of the detector. At the 10-cm source-detector distance, it was found that coincidence summing effects accounted for nearly all of the observed spectrum above 1 MeV and had an appreciable effect below this energy. There were no observable differences in spectra below 1 MeV taken at source-detector distances ≥ 15 cm. Hence, the spectra to be analyzed for low-energy transitions were taken at a 20-cm distance. However, even at this position, there was an appreciable contribution to the spectrum above 1 MeV from coincidence summing effects. Spectra to be analyzed for the presence of the higher-energy transitions were taken at a source-detector separation of 40 cm. These data still showed the presence of summing effects, but they were of minor importance and could readily be taken into account. A beryllium absorber was interposed between the source and the detector to absorb any electrons emitted by the source. Measurements were made in a large cubical graded shield with inside dimensions of 32 in., constructed so as to minimize complications resulting from scattered radiation. The remainder of the spectrometer system consisted of an A-8 linear pulse amplifier coupled to a transistorized 512-channel pulse-height analyzer of conventional design. For counting rates less than 20 000 counts/sec, the integral linearity of the electronic system has been measured to be better than 0.2% of full scale, the differential linearity is of the order of 1%, and the gain stability is better than 0.1 channels/day. Counting rates used in this experiment were of the order of 5000 counts/sec.

Energy calibration of the scintillation spectrometers was accomplished by the method of internal comparison using the 478-keV gamma ray from Be^7. The energies for the pertinent gamma rays in the Ho^{166} spectrum were obtained as follows. Full-energy peaks in a spectrum with a source of $Ho^{166}+Be^7$ were each fit by a method of least-squares to a Gaussian function of the proper width. From this analysis, the positions of the prominent Ho^{166} peaks relative to the Be^7 peak were obtained. These pulse-height positions were then shifted so that the position of the Be^7 peak coincided with its position in a standard pulse-height scale. The positions of the peaks in this standard scale were then compared to a pulse height vs energy curve obtained for this particular spectrometer and the energies were thus obtained. Such a comparison corrects for the nonlinear energy response of NaI(Tl).

A typical pulse-height spectrum obtained from a purified Ho^{166} sample is shown in Fig. 1. For reasons mentioned above, the spectrum was taken at a source-detector distance of 20 cm and is limited to energies below 1 MeV. The spectrum was first unfolded by the method of successive subtraction using response functions for monoenergetic gamma rays calculated[21] for the particular detector and geometry used in this experiment. This analysis yielded relative intensities and energies for some of the major gamma rays and indicated the minimum number of gamma rays needed

[21] R. L. Heath, Proceedings of the Eighth Scintillation Symposium, IRE Trans. Nucl. Sci. NS-9, 3, 294–304 (1962).

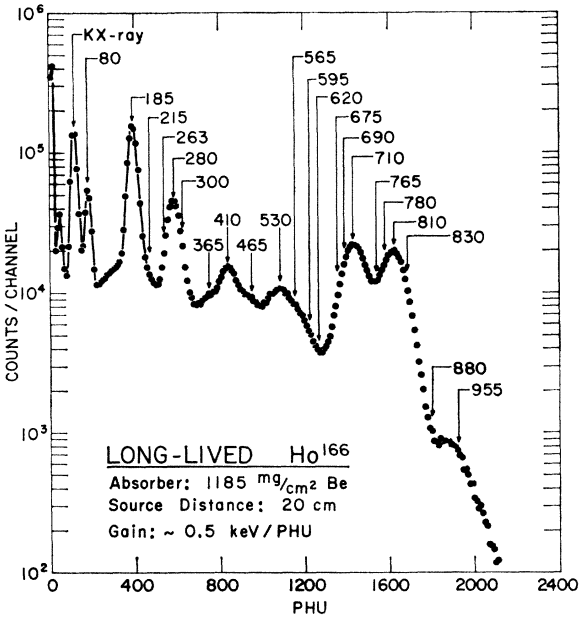

FIG. 1. Gamma-ray spectrum of Ho^{166} showing the energy region below 1 MeV.

to fit the data. The results of the coincidence experiments, however, which are described below, showed the presence of additional low-intensity transitions. Furthermore, four of the weaker transitions observed in the coincidence runs were identified as transitions from lower-spin levels observed[7] in the decay of Tm^{166}. Since the relative intensities of the gamma rays which de-excite these levels should be the same as those observed previously, an attempt was made in subsequent analyses of the data to maintain, as much as possible, these relative intensities. With the additional energy and relative-intensity information obtained from the coincidence measurements, a least-squares analysis was made of the data of Fig. 1. Details of this method are given in reference 21. The fit used calculated response functions for the 23 transitions which had been observed in this energy region. Both the pulse-height positions and intensities of the gamma rays were allowed to vary, subject to those restrictions mentioned above. The least-squares analysis yielded a calculated spectrum which deviated from the experimental spectrum at each point by no more than the statistical uncertainty of that point. It should be pointed out, however, that had there been no information available to supplement the gamma-ray singles spectrum, no meaningful least-squares analysis could have been made. The uncertainties in the intensities and energies of the weaker transitions are relatively large due to the nonuniqueness in the analysis for these gamma rays. The pulse-height positions of the full-energy peaks for all of the 23 transitions are shown in the figure. Figure 2 shows a typical spectrum taken with a stronger source at a source-detector distance of 40 cm. Since the source was located near one wall of the shield, the shape of this spectrum below ≈ 300 keV, when compared to that in Fig. 1, shows the effects of the presence of increased backscattered radiation. Four transitions were observed with energies above 1 MeV. The presence of the 1295-keV gamma ray was indicated also by the coincidence data. Gamma-ray energies and intensities obtained from the analyses are listed in Table I. Absolute transition intensities were obtained by assuming that all of the gamma-ray cascades proceeded through the 80-keV level and that the 80-, 185-, 215-, 263-, 280-, and 300-keV gamma rays were pure $E2$ transitions. Corrections to the intensities of the higher-energy transitions for internal-conversion effects were negligible. Relative intensities for the 215-, 263-, and 300-keV transitions were obtained from the gamma-gamma coincidence measurements and from the electron spectra.

Gamma-gamma coincidence measurements were made using a pair of 3 in.$\times$3 in. NaI(Tl) detectors. Measurements were made in a large graded shield with inside dimensions of 32 in.$\times$32 in.$\times$44 in. All measurements were made at 90° geometry, and the detectors were shielded from one another to reduce the effects of

TABLE I. List of gamma-ray energies, gamma-ray intensities, and transition intensities.

E_γ (keV)	I_γ (%/β^- transition)	I_t (%/β^- transition)
80± 2[abc]	11.6[efg]	100%
185± 3[abc]	90.4[efg]	95.5±6.0
215± 3[bc]	3.5[fg]	4.3±2.4
263± 3[bc]	1.7[fg]	2.0±1.0
280± 5[abc]	29.9[efg]	32.0±3.0
300± 5[bc]	3.4[fg]	3.5±1.8
365± 5[ab]	2.8[ef]	2.8±0.3
410± 5[abc]	15.1[efg]	15.2±1.7
465±10[abc]	1.9[ef]	1.9±0.4 } 5.0±0.5
465±10[b]	3.1[f]	3.1±0.5 }
530± 5[abc]	11.0[efg]	11.0±1.2
565± 5[ab]	7.5[ef]	7.5±1.0
595±10[bd]	0.8[h]	0.8±0.4
620±10[b]	2.5[f]	2.5±0.8
675±10[b] } [a]	4.8[f]	4.8±2.0
690±10[d] }	1.5[h]	1.5±0.8
710± 5[abc]	62.1[ef]	62.1±6.5
765±10[b] } [a]	6.8[f] } [e]	6.8±1.0
780±10[bd] }	3.5[h] }	3.5±1.5
810± 5[abc]	56.2[ef]	56.2±6.0
830± 5[abc]	11.2[fg]	11.2±3.5
880±10[b]	1.0[f]	1.0±0.3
955± 5[ab]	3.3[ef]	3.3±0.5
1135± 5[ab]	0.5[ef]	0.5±0.1
1240± 5[ab]	1.2[ef]	1.2±0.2
1295±10[ab]	0.2[ef]	0.2±0.1
1415± 5[ab]	1.2[ef]	1.2±0.2

[a] Transition observed in gamma-ray singles measurements.
[b] Transition observed in gamma-gamma coincidence measurements.
[c] Transition observed in electron measurements.
[d] Transition inferred from results of the Tm^{166} decay studies of Harmatz *et al.* (reference 7).
[e] Relative intensity determined from gamma-ray singles measurements.
[f] Relative intensity determined from gamma-gamma coincidence measurements.
[g] Relative intensity determined from electron measurements.
[h] Relative intensity inferred from results of Harmatz *et al.* (reference 7).

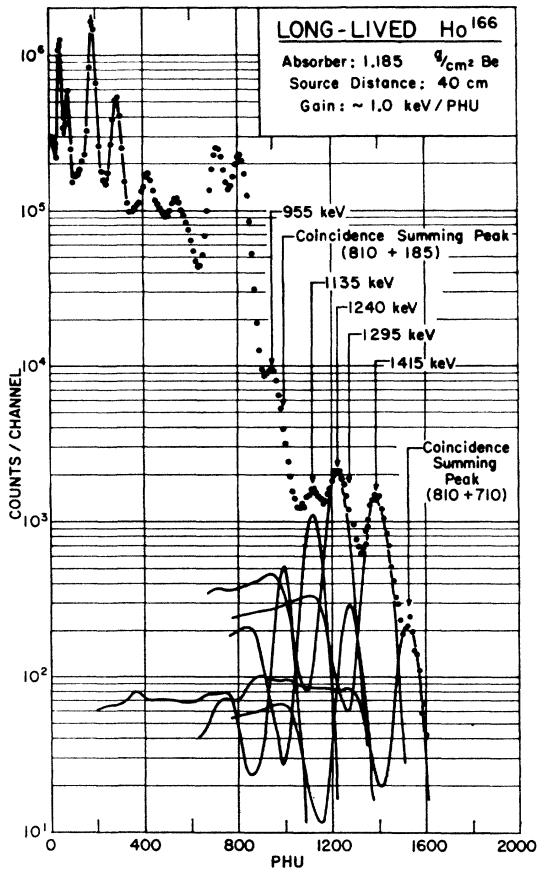

FIG. 2. Gamma-ray spectrum of Ho^{166} showing the high-energy transitions.

coincidences resulting from the scattering of photons between the crystals. The coincidence spectrometer consisted of a single-channel pulse-height analyzer operated in coincidence with a 256-channel transistorized analyzer. Double-differentiated delay-line amplifiers were used on both channels to permit the use of the zero crossover point, characteristic of the pulse shape produced by this amplifier, to derive timing signals for the fast coincidences in the fast-slow coincidence system. With this system, 100% coincidence efficiency for all pulses from 2 to 90 V in amplitude was achieved with a fast resolution of 8×10^{-8} sec. For these measurements, 22 single-channel-analyzer settings of approximately equal width spanned the pulse-height region corresponding to energies between 80 and 980 keV. Coincidence spectra were taken under several different experimental conditions because of difficulties arising from coincidence summing. One set of data was taken at source-detector distances of 15 cm with no absorber over the NaI(Tl) crystals. These data were used in the analysis of the region below 300 keV. The higher energy region, however, was complicated by coincidence summing of low-energy transitions with those of higher energy. For this reason, another set of data was taken at 10 cm with 2-mm Pb absorbers over the face of the crystals. The absorbers served to attenuate the low-energy gamma rays and thus reduced the summing effects. These data were used in analyses of the energy region between 0.3 and 1 MeV. To obtain the coincidence relationships of the transitions with energies above 1 MeV, measurements were made at 20 cm with a 2-mm Pb absorber over the multichannel detector. With this arrangement, spectra were taken in coincidence with the 185- and 280-keV gamma rays.

Each of the coincidence spectra was unfolded by means of the subtraction process, using response functions characteristic of the detector used under the conditions of the experiment. The systematic scanning used in taking the spectra permitted the observation of the variation in intensity of a particular transition as the window of the single-channel analyzer was moved across a small region of the gamma-ray singles spectrum. Thus it was possible to determine if a gamma ray were truly in coincidence with a particular photopeak, or with the Compton distribution associated with higher energy gamma rays.

Representative samples of the coincidence data are presented in Fig. 3. For spectrum No. 1, the single-channel window scanned a region in which contributions from the 955-, 830-, and 810-keV transitions were comparable. The energy and intensity relations of certain of the photopeaks in this spectrum should be noted. On the high-energy side of several of the peaks, there appeared a weaker photopeak. In each case the separation of the two peaks was $\approx$55 keV. This doublet-type structure was observed to exist in the 410–465-keV, the 565–620-keV, and the 710–765-keV photopeak pairs. Furthermore, it was observed that in all the coincidence spectra, the relative intensities of the two members of these photopeak pairs were constant (to within the statistical uncertainties of the data). This behavior can be explained by assuming that each higher energy peak arises from coincidence summing between the corresponding lower energy gamma ray and a K x ray or that it indeed represents a real gamma ray. Since a comparison of the spectra taken with and without Pb absorbers indicated that there was no significant difference in the relative intensity of the members of each photopeak pair, it was concluded that the higher energy peaks did not arise primarily from coincidence summing. Additional evidence which supports this conclusion was provided by spectra (e.g., spectrum No. 2) in which the 810-keV transition was the major photopeak present. In these spectra, there was no evidence for the existence of a peak at 865 keV, even though such a peak would have been observed if its intensity, relative to that of the 810-keV peak, had been as much as 1%. The interpretation of this spectrum, along with the other coincidence data, is that these gamma-ray pairs arose from two higher energy states in Er^{166}, separated by

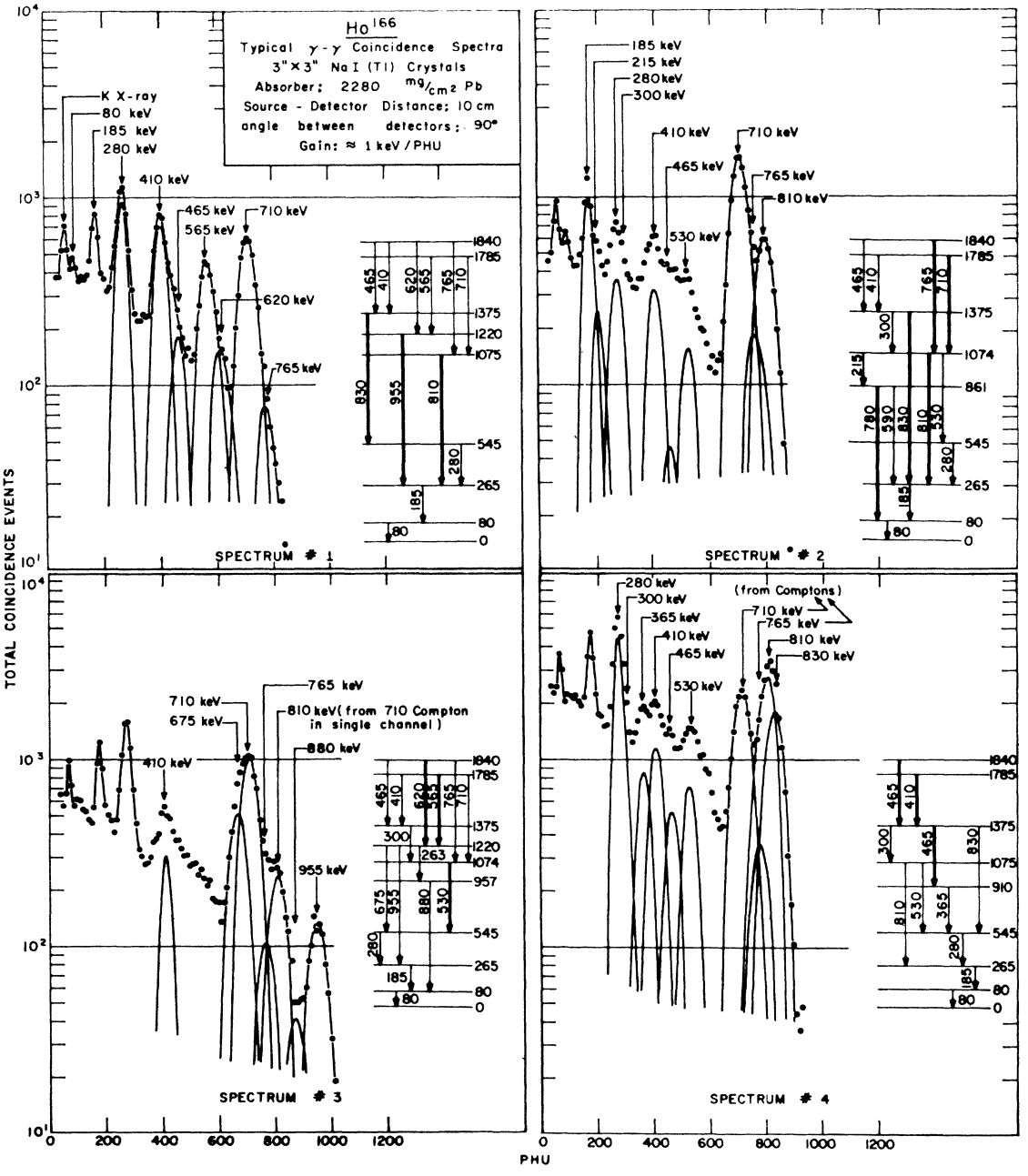

FIG. 3. Typical γ-γ coincidence spectra. Spectra 1, 2, 3, and 4 are coincident with $\approx$40 keV single-channel energy regions centered about 900, 790, 565, and 450 keV, respectively. The heavy lines shown in the partial decay scheme in conjunction with each spectrum represents the transitions whose photopeaks are included in the single-channel windows.

55 keV. Each of these pairs represented transitions from these two states to a different final state in Er^{166}. The partial decay scheme shown in conjunction with the spectrum shows the location of these transitions. Spectrum No. 2 shows the coincidence spectrum obtained with a single-channel window centered about 790 keV. Included in the window were contributions from the 830-, 810-, 780-, 765-, and 710-keV gamma rays. The presence of a 215-keV transition should be noted in the spectrum. This transition was found to be in coincidence with a relatively wide energy region (from about 680 to 790 keV), in which the dominant contributions are from the 710-, 765-, and 780-keV transitions. Spectrum No. 3, taken in coincidence with the region about 565 keV, shows the presence and relative intensities of the 675-, 880-, and 955-keV transitions. Although the 263-keV transition was observed in other coincidence spectra, no meaningful

estimate of its intensity could be obtained from these data. Therefore, one measure of its intensity was obtained by making use of the fact that it is presumably the only transition which populates the level at 957 keV. Since the only two transitions which de-excite this level are the 880- and 690-keV transitions and since the relative intensity of these two gamma rays has been measured by Harmatz *et al.*,[7] one may infer the intensity of the 263-keV gamma ray in this spectrum from the observed intensity of the 880-keV transition. This yields the intensity of the 263-keV transition relative to the intensity of the 955-keV transition which is also observed in this spectrum. The value obtained agreed with that obtained from the electron measurements. Spectrum No. 4, taken in coincidence with an energy region about 450 keV, shows the presence of 410- and 465-keV transitions in relative abundances significantly different from those observed in other coincidence spectra. Furthermore, analyses of spectra taken with single-channel settings adjacent to that of spectrum No. 4 show definite 410–465-keV and 465–465-keV coincidence relationships, indicating the presence of two 465-keV gamma rays. Quantitative analyses of the gamma-ray coincidence and singles data yielded relative intensities for these two gamma rays. The intensities obtained are those listed in Table I. An estimate was made of the relative intensity of the 300-keV transition from the relative intensities of the 830- and 810-keV transitions also present in this spectrum, after correcting for the presence in the single-channel window of the Compton distributions from the 710- and 765-keV gamma rays. The intensity obtained from this measurement also agreed with that obtained from analyses of the electron spectra. Figure 4 shows typical spectra obtained in coincidence with the 185- and 280-keV gamma rays, respectively. The presence of the 1295-keV transition is noted in the insert in the right-hand spectrum. The relative intensity of this gamma ray listed in Table I was obtained from this measurement. The 1240–1295-keV pair represented transitions from the same two high-energy states, separated by 55 keV, which were mentioned in the discussion of Fig. 3.

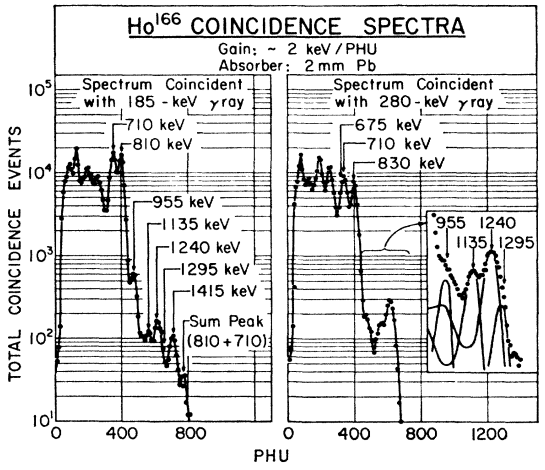

FIG. 4. Gamma-ray spectra coincident with the 185- and 280-keV transitions, respectively, showing the coincidence relationships of the high-energy transitions.

C. Electron Measurements

Electrons emitted in the decay of Ho^{166} were observed with silicon-diode solid-state detectors. The electronic system used with these detectors consisted of an ORNL type Q-2069C low-noise high-gain linear-amplifier system with a multichannel analyzer. Two detectors were used in these measurements. One of these was a lithium-drift detector[22] while the other was a surface-barrier detector.[23] The lithium-drift detector had a depletion depth equivalent to the range of an 1100-keV electron and a window thickness equivalent to the range of a 100-keV electron. Hence the K- and L-shell conversion electrons from the 80-keV transition did not penetrate this layer. Energy calibration and resolution measurements were made using the conversion electrons from a source of Bi^{207}. The detector was cooled to $-70°C$ by means of an alcohol-dry-ice bath in contact with the mounting bracket of the detector. At this temperature, the resolution (FWHM) at 480 keV was about 8 keV.

A typical electron spectrum taken using the lithium-drift detector is shown in Fig. 5. The lower curve in the figure shows the spectrum from the gamma radiation alone. The statistics of this background run are much poorer than those of the upper curve due to the difference in the length of the two runs. It is seen, however, that the gamma response of this detector masked the conversion lines from many of the transitions. While detectors of this type have inherently good resolution characteristics, and thus provide an excellent means for observing conversion electrons, the gamma-ray response associated with thick depletion layers can in some instances present serious problems. The spectrum does, however, show the conversion lines from the stronger transitions, particularly those having energies above the Compton edge of the 810-keV transition. Of particular interest are the relative heights of the K-conversion lines for the 710- and 830-keV transitions. From the relative intensities of these transitions, and from the relative K-conversion coefficients[24] for various assumed multipolarities, one may show that the 710- and 810-keV transitions are of different multipolarities, the 810-keV transition having the higher multipolarity. A similar analysis of the data on the 410- and 530-keV transitions shows that the 530-keV transition has the

[22] Measurements using the lithium-drift detector were made at ORNL using a detector developed by Blankenship and Ryan of that laboratory.

[23] Purchased from ORTEC.

[24] L. A. Sliv and I. Band, Leningrad Physico-Technical Institute Report, 1956 [translation: Report 57 ICCK1, issued by the Physics Department, University of Illinois, Urbana, Illinois (unpublished)].

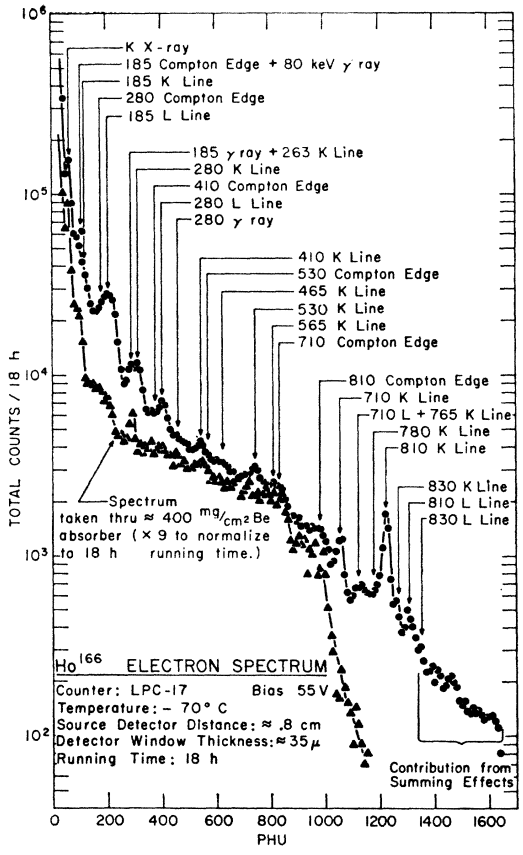

FIG. 5. Electron spectrum of Ho^{166} taken with a lithium-drift detector having a depletion thickness of ≈1.75 mm.

higher multipolarity. Although the L lines for the 810- and 710-keV gamma rays are also present in the spectrum, theoretical K/L ratios are not sensitive enough in these energy regions to distinguish between an $E2$ and an $M1$ assignment for the 810-keV gamma ray and between an $E1$ and an $E2$ assignment for the 710-keV transition. A comparison of conversion-line intensities of the 410-, 530-, 710-, and 810-keV transitions with that of the 185-keV $E2$ transition,[7] indicates that the 410- and 710-keV gamma rays are predominantly $E1$ and the 530- and 810-keV transitions are predominantly $E2$. These multipolarity assignments for the 710- and 810-keV transitions agree with those of Postma *et al.*,[25] obtained from studies of the gamma rays from aligned Ho^{166} nuclei. The relative abundance of conversion electrons from the 830-keV gamma ray is consistent with the relative intensity of the 830-keV transition observed in the gamma-gamma coincidence measurements if this transition is $E2$. The absence of a significant peak in the electron spectrum representing the K-line from the 565-keV transition indicates that this gamma ray is probably $E1$.

The surface-barrier detector was operated at a bias such that the depletion depth was equivalent to the range of a 300-keV electron. The window width was of the order of a few keV. Due to the thin depletion depth, the efficiency for the detection of gamma rays was sufficiently low that no difficulties arose from this effect. Figure 6 shows a typical spectrum taken with this detector. As may be seen in the figure, the noise level of the detector and amplifier system was such that no meaningful data could be taken below ≈20 keV. To investigate contributions to these data from summing effects, runs were taken at three different source-detector separations. Contributions from gamma-ray detection were measured by placing an absorber over the source. The results of these measurements showed that the background in Fig. 6 was primarily due to these two effects and their contributions were taken into account in the analysis of the data. The spectrum clearly shows the K lines from the 215-, 263-, and 300-keV transitions. Intensities for these transitions, relative to that of the 185-keV transition, were obtained by assuming a shape for the background and by assuming that the transitions were $E2$. Due to the presence of the background, the uncertainties in these values are large. The 9-keV width of the peaks in the spectrum when compared with the 8.7-keV width inherent to this detector and amplifier system, places an upper limit of 200 $\mu g/cm^2$ on the thickness of the source. Such a thickness, however, would be expected to seriously degrade the spectrum at very low energies (<35 keV). In spite of the degraded low-energy portion of this spectrum, it was nevertheless possible to establish an upper limit for the end-point energy of the most intense β^- branch. This was accomplished in the following manner. The shape of allowed beta distributions were calculated for several end-point energies. These distributions, shown on Fig. 6, were normalized

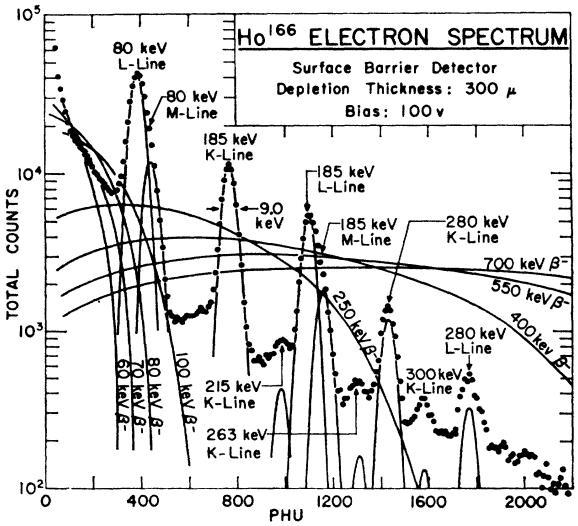

FIG. 6. Electron spectrum of Ho^{166} taken with a surface-barrier detector.

[25] H. Postma, A. R. Miedema, and M. C. Eversdijk Smulders, Physica 25, 671 (1959).

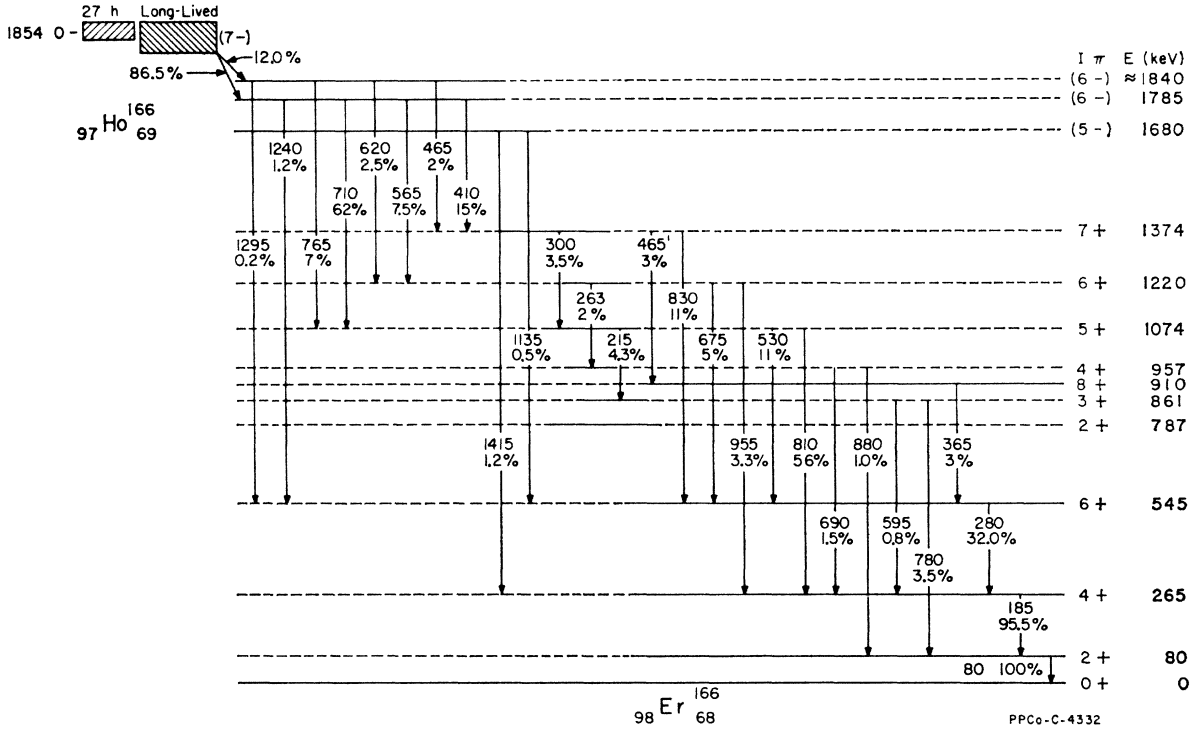

FIG. 7. Proposed decay scheme for the long-lived Ho^{166} isomer.

to the data using the observed intensity of the 80-keV L line, the branching ratio for this beta transition (obtained from gamma-ray intensity data), and the fact that all gamma cascades proceed through the 80-keV level. A comparison of these calculated curves with the experimental data of Fig. 6 shows that the maximum end-point energy for this transition must be less than ≈ 65 keV. A lower limit of ≈ 55 keV for the endpoint energy of this transition is provided by the fact that a level in Er^{166} is found to lie ≈ 55 keV above the level fed by the most intense branch of the beta decay. Hence, it is believed that the end-point energy of the main beta group must lie between 55 and 65 keV.

III. LEVEL SCHEME AND DISCUSSION OF EXPERIMENTAL RESULTS

A decay scheme for the long-lived Ho^{166} isomer, based on the gamma-ray and electron measurements presented above, is shown in Fig. 7. The level structure of Er^{166} shown in this figure exhibits the familiar level sequence associated with highly deformed even-even nuclei. In further discussions of the level scheme, the notation of Davydov and Filippov[2] will be used. This notation denotes the first 2+ level as the ^{12} level, the second 2+ level as ^{22}, etc.

The ^{12} and ^{22} levels in Er^{166}, with energies of 80 and 787 keV, respectively, have been observed previously in studies[8–15] of the decay of 27-h Ho^{166}. Furthermore, the ^{14}, ^{16}, ^{13}, and ^{24} levels at 265, 545, 861, and 957 keV, respectively, have been observed in the studies of the decay of Tm^{166}.[5–7] Although transitions to and from the ^{22} level at 787 keV were not observed in the present work, the level was included in Fig. 7 for the sake of completeness.

The level at 910 keV was observed in the present study to depopulate through a transition to the ^{16} level at 545 keV. No other transitions from this level were observed. A spin of 8 was assigned to this level since it feeds only the ^{16} level and since an 8+ state of approximately this energy is predicted by collective-structure considerations. The level at 1074 keV populates levels with spins and parities of 3+, 4+, and 6+. No direct feeding of either the ^{12} or the ^{22} level from the state at 1074 keV was observed. Hence, the level was assigned a spin and parity of 5+. If the parity were odd, one would expect almost no feeding of the 3+ state since the transition would then be $M2$ and would not be expected to compete with the $E1$ transitions to the ^{14} and ^{16} states. An additional argument for an even parity state lies in the fact that both the 810- and 530-keV transitions are predominantly $E2$. The level at 1220 keV was observed to populate only the ^{14}, ^{24}, and ^{16} states. Presumably, the ^{15} state is also fed, but with a sufficiently low intensity that the transition was not observed in this experiment. No transitions to the ^{13} level were observed. Therefore, the level at 1220 keV was assigned a spin of 6. An even parity was assigned on the basis of relative-intensity considerations. The level at 1374 keV de-excites to the ^{16}, ^{18}, and ^{15} states. Since no feeding of either the ^{14} or the ^{24} level was in

evidence, a spin assignment of 7 was made to the state. The intensity of the 465-keV ($^{1}7 \rightarrow {}^{1}5$) transition relative to that of the 830-keV ($^{1}7 \rightarrow {}^{1}6$) transition and the presumed $E2$ character of the 830-keV transition indicated a positive parity for this $^{1}7$ level. Further arguments for the spin and parity assignments to the levels at 1074, 1220, and 1374 keV lie in the fact that such states are also predicted from collective-structure considerations to lie at approximately these energies. From the existence of the 1135- and 1415-keV gamma rays and their observed coincidence relationships, a level was placed at 1680 keV. A 5− assignment was made to this level since it de-excites only to the $^{1}6$ and $^{1}4$ states. This level may be fed either by a direct beta transition or by gamma-ray de-excitation of a higher level. At present the experimental evidence does not indicate which of these two possibilities is the correct one. The level at 1785 keV appears to de-excite by $E1$ radiation to the $^{1}6$, $^{1}5$, $^{2}6$, and $^{1}7$ levels. No feeding of the $^{1}4$ level is observed. This level has therefore been assigned a spin and parity of 6−. Finally, the level at 1840 keV also appears to feed only the $^{1}6$, $^{1}5$, $^{2}6$, and $^{1}7$ states with nearly the same intensity ratios as those observed in the transitions from the level at 1785 keV. This, and the fact that no direct transitions to the $^{2}4$ level are observed, lead to a 6− assignment for this state as well.

The three states at 1680, 1785, and 1840 keV appear to arise from nucleon configurations different from that of the ground state. There are several possible configurations which can give rise to high-spin states in Er^{166} with odd parity. Such states can arise from the excitation of either a neutron or a proton. Some information concerning the states available to the 98th neutron is provided by a knowledge of the ground states of the neighboring odd-N nuclei, $Er_{97}{}^{165}$ and $Er_{99}{}^{167}$. The ground-state assignments have been reported[26] to be 5/2− and 7/2+, respectively. Therefore, the 97th and 99th neutrons are presumably in the Nilsson orbits [523]5/2− and [633]7/2+, respectively. If in $Er_{98}{}^{166}$, the 98th neutron is excited to the [633]7/2+ state, the two unpaired neutrons can give rise to two distinct rotational bands. One of these bands is based on a 1− intrinsic state, and the other is based on a 6− state. Similarly, information concerning states available to the 68th proton is given by a knowledge of the ground states of the neighboring odd-Z nuclei, $_{67}Ho^{165}$ and $_{69}Tm^{167}$. From such information, the 67th and 69th protons are presumed to be in the Nilsson orbits [523]7/2− and [411]1/2+, respectively. Thus if the 68th proton in Er^{166} is excited to the [411]1/2+ state, the two unpaired protons can yield two separate rotational bands, one based on a 3− level and one based on a 4− level. There are, therefore, at least four configurations that may give rise to these high-spin negative-parity states in Er^{166}.

[26] B. R. Mottelson and S. G. Nilsson, Kgl. Danske Videnskab. Selskab, Mat.-Fys. Skrifter 1, No. 8 (1959).

The two isomers of the Ho^{166} parent presumably arise from the coupling of the unpaired 67th proton, in a [523]7/2− state, and the 99th neutron, in a [633]7/2+ state. These two nucleons can give rise to a 0− and a 7− state. The 27-h level has been shown[11,27,28] to have spin 0. The first-forbidden nature of the beta transitions from this state to even-parity states in the daughter suggests an odd parity. Therefore, the long-lived state is probably the 7− level. From spin and parity considerations only, beta decay from the 7− level to the 6− levels should be of an allowed character. To consider the K-selection rules and the asymptotic selection rules one must examine the decay more closely. If the final state were either of the two states resulting from neutron excitation, the transition would occur between a [523]5/2− neutron and a [523]7/2− proton. Such a decay would satisfy all the asymptotic selection rules[29] for allowed transitions. As mentioned previously, two possibilities exist for 6− states resulting from neutron excitation. One of these is a $K=1$ rotational state based on a 1− intrinsic level and the other is the ground state of a $K=6$ rotational band. An allowed beta transition to the former state from the spin-7 state in Ho^{166} would have a K-hindrance factor of 5. A similar transition to the $K=6$ state would satisfy all the requirements for allowed transitions and would therefore be expected to have a logft value of approximately 5. If, on the other hand, the final state were the result of proton excitation, the beta decay would be a transition between a [633]7/2+ neutron and [411]1/2+ proton. The two 6− levels from proton excitation would be a $K=3$ rotational level and a $K=4$ rotational level. Allowed beta transitions to either of these levels would be K forbidden and hindered due to violation of the asymptotic selection rules. Beta decay to the $K=4$ level might be expected to have a logft value in the range of 10 to 12, while that to the $K=3$ level should be somewhat higher. If the 5− level is populated by direct beta feeding, the decay should be second forbidden. Furthermore, if the level is one of those resulting from proton excitation (i.e., either $K=3$ or 4), the beta transition should be K forbidden. One would, therefore, expect the logft value for this transition to lie in the range from 13 to 16.

The half-life of the long-lived Ho^{166} isomer has been recently measured[30] to be $(9\pm2)\times10^{4}$ years. If the endpoint energy for the beta transition to the 1785-keV level is 57 keV, a value consistent with the measurements described in Sec. II C, the logft for this transition is approximately 10.5. Such a value is consistent with the assumption that the 1785-keV state has $K=4$ and results from a proton excitation. The 4− and 5− levels of this band would lie at lower excitation energies.

[27] L. S. Goodman, W. J. Childs, R. Marrus, I. P. K. Lindgren, and A. Y. Cabezas, Bull. Am. Phys. Soc. 5, 344 (1960).
[28] W. J. Childs and L. S. Goodman, Phys. Rev. 122, 591 (1961).
[29] G. Alaga, Nucl. Phys. 4, 625 (1957).
[30] K. T. Faler and B. Keisch (private communication).

Low-energy $E2$ transitions to these states from the 6− state might not be expected to compete with the higher energy $E1$ transitions to the high-spin members of the ground-state band even though the $E1$ transitions would be hindered due to violation of the asymptotic selection rules[26] for gamma emission. If the end-point energy of the higher energy beta transition is 57 keV, the end-point energy for the beta transition to the state at 1840 keV would then be of the order of 2 keV. This would give a logft of about 5 for the decay. This state, then, could be the $K=6$, 6− state resulting from neutron excitation. The $K=1$, 1− state resulting from neutron excitation has been reported[14,15] to lie at 1830 keV. Further study is believed to be necessary before definite nucleon configuration assignments can be made to these two levels. If the state at 1680 keV is fed by beta decay, the logft for this decay is ≈ 13.5. No attempt was made to make any configuration assignment to this state.

From the suspected end-point energies of the beta groups and from the energies of the levels fed by the beta decay, it appears that the 7− state in Ho^{166} lies about 1840 keV above the ground state of Er^{166}. Graham *et al.*[11] have reported that the 27-h level in Ho^{166} lies 1854±5 keV above the ground state of Er^{166}. The indication, therefore, is that the 9×10^4-yr level lies approximately 10 keV below the 27-h level and is hence the ground state of Ho^{166}. This result depends sensitively upon the beta end-point energies.

IV. INTERPRETATION IN TERMS OF AN ASYMMETRIC-ROTATOR MODEL

The observed properties of the low-lying states of a large number of even-even nuclei appear to be well described as rotational excitations of an axially asymmetric nuclear configuration.[2,3] Because of the lack of detailed experimental evidence on the properties of the high-spin levels of these nuclei, the comparison of this "asymmetric-rotator" model with experiment has usually been restricted to the low-spin levels ($J\lesssim 4$). Since this model not only "predicts" the energies and angular momenta of the nuclear states, but the transition probabilities between them as well, it was decided to apply it to the observed Er^{166} levels.

While the quantum mechanical treatment of the asymmetric rotator has been discussed elsewhere,[31,32] it is believed that a brief description of the essential points of this model will aid in an understanding of its application to this specific case. This discussion follows that of references 3 and 32.

The Hamiltonian which describes the rotational motion has the form:

$$(h/\hbar^2)(AQ_A^2+BQ_B^2+CQ_C^2). \qquad (1)$$

The Q_i are operators for the components of the rotational angular momentum about the three principal axes and are expressed in terms of a coordinate system fixed in the nucleus. The rotational constants A, B, and C are related to the corresponding moments of inertia through expressions of the form $A=\hbar/4\pi I_A$, etc.

In the asymmetric-rotator model as originally introduced,[2,33] the moments of inertia were assumed to have the form $I_\lambda \propto \sin^2(\gamma-\frac{2}{3}\pi\lambda)$, $\lambda=1, 2, 3$, as given by the hydrodynamical model.[34] However, the form of the model employed here is that of later treatments,[3,35] in which the three principal moments of inertia are allowed to be arbitrary. We label the principal axes of the nuclear system in such a manner that the relation $A\geq B\geq C$ holds. As B ranges from A to C, the rotator ranges between the extremes of an oblate and a prolate spheroid, respectively. The rotational constants A, B, and C may be used to define an asymmetry parameter k, where

$$k=(2B-A-C)/(A-C).$$

The energy levels of the rotator are determined from the eigenvalue equation

$$\frac{hC}{\hbar^2}\left(\frac{A}{C}Q_A^2+\frac{B}{C}Q_B^2+Q_C^2\right)\psi=hC\epsilon_0\psi, \qquad (2)$$

where ϵ_0 is the energy expressed in units of hC. The energy eigenvalues of (2) may be written in the form[32]

$$2\epsilon_0=J(J+1)[(A/C)+1]+[(A/C)-1]E_\tau, \qquad (3)$$

where E_τ is a function of J, τ, and k only. Tables of this function calculated for a wide range of these parameters have been published.[32] τ is an integer which labels the $(2J+1)$ levels of spin J. In terms of the numbers K_{-1} and K_{+1}, which give the values of the asymmetry parameter k for the limiting prolate and oblate tops, respectively, τ may be expressed as $(K_{-1}-K_{+1})$. Since the symmetry conditions discussed by Bohr[34,36] require that these limiting projection numbers K_{-1} and K_{+1} be even integers, the number of allowed values of τ, and hence the number of possible energy levels, is considerably reduced. The values of τ, as well as the values of K_{-1} and K_{+1}, appropriate to the observed rotational levels of Er^{166} are given in Table II.

The subscript, 0, in Eqs. (2) and (3) indicates that the effects of the rotation-vibration interaction have not been taken into account. The inclusion of the rotation-vibration interaction yields, to the first order, the following expression for the energy:

$$\epsilon\equiv E/hC=\epsilon_0-b\epsilon_0^2, \qquad (4)$$

[31] G. Herzberg, *Infrared and Raman Spectra* (D. Van Nostrand Company, Princeton, New Jersey, 1945).
[32] C. H. Townes and A. L. Schawlow, *Microwave Spectroscopy* (McGraw-Hill Book Company, Inc., New York, 1955).
[33] C. Marty, Nucl. Phys. **1**, 85 (1956).
[34] A. Bohr and B. R. Mottelson, Kgl. Danske Videnskab. Selskab, Mat.-Fys. Medd. **27**, No. 16 (1953).
[35] A. S. Davydov, N. S. Rabotnov, and A. A. Chaban, Nucl. Phys. **17**, 169 (1960).
[36] A. Bohr, Kgl. Danske Videnskab. Selskab, Mats.-Fys. Medd. **26**, No. 14 (1952).

TABLE II. Comparison of the calculated Er^{166} rotational levsel with those observed experimentally. Parameters used in the calculation are $k=-0.96$, $A/C=17.14$, $hC=11.62$ keV, $b=6.3\times10^{-4}$ keV^{-1}. The first column denotes the level. The second column lists the value of τ appropriate to the level. The third column gives the limiting values of the projection quantum number for the prolate and oblate symmetric tops. The fourth and fifth columns give the calculated and observed energies, respectively.

Level	τ	K_{-1}, K_{+1}	Calculated energy (keV)	Observed energy (keV)
1^2	-2	0, 2	80.6	80.6[a]
1^4	-4	0, 4	265.1	265.1[a]
1^6	-6	0, 6	545.6	545.3[a]
2^2	$+2$	2, 0	786.8	787.1[a]
1^3	0	2, 2	860.1	860.6[a]
1^8	-8	0, 8	909.8	910
2^4	0	2, 2	957.6	957.2[a]
1^5	-2	2, 4	1075.8	1074
2^6	-2	2, 4	1219.3	1220
1^7	-4	2, 6	1375.6	1374

[a] Energies reported by Jacob *et al.*[5]

where b is a measure of the strength of this interaction.

From an inspection of Eqs. (3) and (4), it is apparent that four parameters (A/C, k, hC, and b) are required to determine the energies of all the collective rotational states. In the application of the model to a specific case, one attempts to find a set of parameters that will reproduce the observed level structure. A detailed discussion of methods for determining a set of such parameters from experimental data has been given by Mallmann.[3] From an analysis of the observed[5] low-spin levels of Er^{166}, Mallmann derived the following parameters: $k=-0.96$, $A/C=17.14$, $hC=11.62$ keV, and $b=6.3\times10^{-4}$ keV^{-1}. These parameters were used in Eqs. (3) and (4) to determine the positions of the Er^{166} levels. The values of E_τ in Eq. (3) for the higher spin levels were obtained from the table given in reference 32. The results of the calculation of the energies of the collective rotational levels in Er^{166} are summarized in Table II. The fact that, in this model, $k=-0.96$ indicates that Er^{166} behaves much like a prolate symmetric top.

In order to calculate the gamma-ray intensities, it is necessary to obtain wave functions. It should be pointed out that, in the calculation of the relative-transition probabilities, the rotation-vibration effects are neglected. Since these effects are small, it is expected that the errors introduced by the neglect of these effects will be for all practical purposes small. The rotational portion of the wave function which describes the nth state of spin J may be expanded in the series:

$$\psi_{nJ,M}=\sum_K A_K({}^nJ)\psi_{JMK}, \tag{5}$$

where the sum goes over all even integers $\leq J$. The basis functions ψ_{JMK}, which incorporate Bohr's symmetry conditions, are the wave functions for a (prolate) symmetric top and have the form

$$\psi_{JMK}=\left[\frac{1}{2(1+\delta_{K,0})}\left(\frac{2J+1}{8\pi^2}\right)\right]^{1/2}[D_{MK}{}^J+(-)^JD_{M-K}{}^J],$$

where K is the projection of the angular momentum upon the axis of symmetry of the top. The $D_{MK}{}^J$ functions are the solutions of the symmetric-top wave equation. The coefficients A_K in (5) may be evaluated by substituting the wave function (5) into the eigenvalue equation (3) and taking matrix elements of the resulting expression with the function $D_{M'K'}{}^{J'*}$. The resulting equations, together with the normalization condition $\sum_K|A_K|^2=1$, are sufficient to determine the A_K (to within an arbitrary phase factor). In carrying out this operation, however, it is convenient to express the Hamiltonian in terms of raising and lowering operators (Q_+ and Q_-). We set $Q_\pm=Q_C\pm iQ_B$. In terms of these operators, the Hamiltonian for the rotational motion becomes

$$H^R=\frac{1}{4}\left(1-\frac{B}{C}\right)(Q_+{}^2+Q_-{}^2)+\frac{1}{4}\left(1+\frac{B}{C}\right)(Q_+Q_-+Q_-Q_+)+\frac{A}{C}Q_A{}^2.$$

By analogy with similarly defined operators,[37] the effect of the operation of the $Q_\pm$ upon a spherical-top wave function $D_{MK}{}^J$ is given by

$$Q_\pm D_{MK}{}^J=\hbar[(J\mp K)(J\pm K+1)]^{\frac{1}{2}}D_{MK\pm1}{}^J.$$

From these relations, together with the relation

$$Q_A{}^2D_{MK}{}^J=K^2\hbar^2D_{MK}{}^J$$

and the orthogonality of the D functions, the matrix elements and hence the expansion coefficients may be calculated.

From the coefficients A_K for the various states, and hence the rotational portion of their wave functions, the intensities of the gamma-ray transitions between various states may be calculated. Since the collective rotational excitations of the ground-state configuration have the same parity, $E1$, $M2$, $E3$, etc., transitions between these states cannot occur. In considering the relative transition intensities in this model, we compare only their $E2$ components. If the observed gamma-ray transitions contain some $M1$ admixture, the calculated intensities may not provide a realistic comparison with the experimental data. The intensity of an $E2$ transition is related to the reduced transition probability $B(E2)$ through the equation[38]

$$T_\gamma=1.23\times10^{-2}(E_\gamma)^5B(E2)\ \text{sec}^{-1}, \tag{6}$$

[37] M. E. Rose, *Elementary Theory of Angular Momentum* (John Wiley & Sons, Inc., New York, 1957).

[38] K. Alder, A. Bohr, T. Huus, B. R. Mottelson, and A. Winther, Rev. Mod. Phys. **28**, 432 (1956), Eq. (IV.3).

TABLE III. Comparison of calculated gamma-ray relative intensities with the experimental relative intensities. In addition to the four parameters used in the calculation of the energy level structure (Table II), two additional parameters, $k_0=2.28\times10^{-24}$ cm^2 and $r=+0.18$, were used. Comparisons were made only between those transitions from common levels.

Transition $(I_i \to I_f)$	E_γ (keV)	$B(E2; I_i \to I_f)$ ($e^2\times10^{-48}$ cm^4) "interband"	"intraband"	T_γ[a] (10^8 sec^{-1})	Relative intensity (calculated)	(experimental)
$^{7} \to {}^{8}$	465	0.073		194	0.14	0.28±0.06
$^{7} \to {}^{6}$	154		0.536	5.7	0.004	[b]
$^{7} \to {}^{6}$	830	0.0292		1406	1.00	...
$^{7} \to {}^{5}$	300		1.37	410	0.29	0.31±0.18
$^{6} \to {}^{8}$	311	0.0199		7.1	0.013	[b]
$^{6} \to {}^{6}$	675	0.0721		1230	2.25	1.3 ±0.7
$^{6} \to {}^{4}$	955	0.0055		546	1.00	...
$^{6} \to {}^{5}$	146		0.714	5.8	~0.01	[b]
$^{6} \to {}^{4}$	263		1.23	190	0.35	0.6 ±0.4
$^{5} \to {}^{6}$	530	0.0595		306	0.18	0.18±0.03[c]
$^{5} \to {}^{4}$	117		0.960	2.6	0.002	[b]
$^{5} \to {}^{4}$	810	0.0392		1670	1.00	...
$^{5} \to {}^{3}$	215		0.993	53.2	0.032	0.08±0.06
$^{4} \to {}^{6}$	410	0.0134		19.6	0.014	[b]
$^{4} \to {}^{3}$	96		1.38	1.4	~0.001	[b]
$^{4} \to {}^{4}$	690	0.0720		1397	1.00	...
$^{4} \to {}^{2}$	170		0.615	10.6	~0.01	[b]
$^{4} \to {}^{2}$	880	0.0115		732	0.524	0.56[d]
$^{3} \to {}^{4}$	595	0.0401		368	1.00	...
$^{3} \to {}^{2}$	74		1.86	0.5	~1×10^{-3}	[b]
$^{3} \to {}^{2}$	780	0.0543		1940	5.3	5.0[d]
$^{2} \to {}^{4}$	522	0.0037		17.5	~0.01	[b]
$^{2} \to {}^{2}$	707	0.0583		1270	1.14	1.1[d]
$^{2} \to {}^{0}$	787	0.0304		1120	1.000	...

[a] Calculated using Eq. (6). [b] Not observed. [c] Relative intensity used to obtain parameters. [d] Intensities reported by Jacob *et al.*[5]

where E_γ is in keV and $B(E2)$ in units of $e^2\times10^{-48}$ cm^4. The reduced transition probability for an $E2$ transition between the states ^nJ and $^mJ'$ may be expressed in the form[3]

$$B(E2; {}^nJ \to {}^mJ') = e^2k_0^2 \sum_{\mu,M'} \left| \left\langle \psi_{nJ,M} \right| D_{\mu 0}{}^2 + \frac{r}{\sqrt{2}}(D_{\mu 2}{}^2 + D_{\mu -2}{}^2) \left| \psi_{mJ',M'} \right\rangle \right|^2. \quad (7)$$

In this expression two additional parameters, the intrinsic quadrupole moments k_0 and k_2, appear. They represent expectation values of the quantities

$$\sum_{i=1}^{q}(3z_i^2 - r_i^2) \quad \text{and} \quad \sum_{i=1}^{q}(x_i^2 - y_i^2),$$

respectively, over the intrinsic wave function of the states. In terms of k_0 and k_2, the parameter r is $(k_2/k_0)\sqrt{2}$. The parameters k_0 and r were determined from the measured lifetime[39] of the 80-keV (^{2}) state and the measured relative intensity of the 530-keV ($^5 \to {}^6$) and the 810-keV ($^5 \to {}^4$) transitions. Values of 2.28×10^{-24} cm^2 and $+0.18$ were obtained for k_0 and r, respectively. While expressions for $B(E2)$ values for some of the transitions have been given by Mallmann,[3] expressions for the $B(E2)$ values for the $^n7 \to {}^m6$, $^n7 \to {}^m5$, $^n6 \to {}^m6$, $^n6 \to {}^m8$, and $^n7 \to {}^m8$ transitions, required in this comparison, have not previously been presented. These expressions are given in the Appendix. A comparison of the results of the calculations of the gamma-ray relative intensities with the experimental results is summarized in Table III. It is interesting to note that the calculated $B(E2)$ values may be arranged into two groups. The first group consists of what would be called "intraband" transitions (in the terminology of the unified model) and has $B(E2)$ values which are of the order of magnitude of unity (in units of $e^2\times10^{-48}$ cm^4). The second group corresponds to the "interband" transitions and has $B(E2)$ values which are typically two orders of magnitude smaller than those of the first group. The agreement between these calculations and the experimental results is considered to be quite good. It appears that the asymmetric rotator model provides a good description of the experimental data presently available concerning the low-lying positive parity states of Er^{166}.

[39] F. K. McGowan, Phys. Rev. **80**, 923 (1950).

ACKNOWLEDGMENTS

The authors are indebted to E. H. Turk of the Chemistry Section at the Materials Testing Reactor for his many hours of work in purifying the sources used in this experiment, to Dr. K. T. Faler for supplying us with the results of the half-life measurement prior to publication, to Dr. K. T. Hecht of the Physics Department, University of Michigan, for an interesting discussion concerning the nucleon configurations, and to the staff of ORNL, particularly C. Ryan and J. Blankenship of the Instrument Group and Dr. A. Chetham-Strode of the Chemistry Group for their assistance in making the measurements using the lithium-drift detector.

APPENDIX. EXPRESSIONS FOR $B(E2)$ VALUES FOR TRANSITIONS BETWEEN CERTAIN STATES OF AN ASYMMETRIC ROTATOR

In the notation of Eq. (5), the rotational portion of the wave function for the nth state of spin J of an asymmetric rotator may be written in the form

$$\psi_{n_{J,M}}=\sum_K A_K({}^nJ)\psi_{JMK}.$$

One may express the $B(E2)$ values for the respective transitions in terms of these coefficients A_K, the intrinsic quadrupole moment k_0, and the ratio r. In the following expressions, the $B(E2)$ value expressed in units of $(ek_0)^2$ is denoted by the symbol $b(E2)$.

$$\begin{aligned}
b(E2;\,{}^n6\rightarrow{}^m6)=&\,(2/385)\{7A_0({}^m6)A_0({}^n6)+5A_2({}^m6)A_2({}^n6)-A_4({}^m6)A_4({}^n6)-11A_6({}^m6)A_6({}^n6)\\
&-(r/\sqrt{2})[(A_0({}^m6)A_2({}^n6)+A_0({}^n6)A_2({}^m6))2(35)^{1/2}+(A_2({}^m6)A_4({}^n6)+A_4({}^m6)A_2({}^n6))3(5)^{1/2}\\
&+(A_6({}^m6)A_4({}^n6)+A_4({}^m6)A_6({}^n6))(11)^{1/2}]\}^2,\\
b(E2;\,{}^n6\rightarrow{}^m8)=&\,(17/13)b(E2;\,{}^m8\rightarrow{}^n6)=(1/21\,840)\{56A_0({}^n6)A_0({}^m8)\sqrt{3}+90A_2({}^n6)A_2({}^m8)\\
&+A_4({}^n6)A_4({}^m8)12(33)^{1/2}+A_6({}^n6)A_6({}^m8)2(273)^{1/2}+(r/\sqrt{2})[A_0({}^n6)A_2({}^m8)12(35)^{1/2}\\
&+A_2({}^n6)A_0({}^m8)4(105)^{1/2}+A_2({}^n6)A_4({}^m8)6(165)^{1/2}+A_4({}^n6)A_2({}^m8)6(5)^{1/2}\\
&+A_4({}^n6)A_6({}^m8)2(3003)^{1/2}+A_6({}^n6)A_4({}^m8)2\sqrt{3}+A_6({}^n6)A_8({}^m8)4(1365)^{1/2}]\}^2,\\
b(E2;\,{}^n7\rightarrow{}^m5)=&\,(11/15)b(E2;\,{}^m5\rightarrow{}^n7)=(1/546)\{12A_2({}^n7)A_2({}^m5)+A_4({}^n7)A_4({}^m5)(66)^{1/2}\\
&+r[A_2({}^n7)A_4({}^m5)+A_4({}^n7)A_2({}^m5)(66)^{1/2}+A_6({}^n7)A_4({}^m5)(143)^{1/2}]\}^2,\\
b(E2;\,{}^n7\rightarrow{}^m6)=&\,(13/15)b(E2;\,{}^m6\rightarrow{}^n7)=(1/420)\{A_2({}^n7)A_2({}^m6)3(5)^{1/2}+A_4({}^n7)A_4({}^m6)2(33)^{1/2}\\
&+A_6({}^n7)A_6({}^m6)3(13)^{1/2}+(r/\sqrt{2})[5A_4({}^m6)A_2({}^n7)+A_4({}^n7)A_6({}^m6)\sqrt{3}-A_2({}^n7)A_0({}^m6)6(7)^{1/2}\\
&-A_4({}^n7)A_2({}^m6)(165)^{1/2}-A_6({}^n7)A_4({}^m6)(143)^{1/2}]\}^2,\\
b(E2;\,{}^n7\rightarrow{}^m8)=&\,(17/15)b(E2;\,{}^m8\rightarrow{}^n7)=(1/1260)\{A_2({}^n7)A_2({}^m8)2(30)^{1/2}+A_4({}^n7)A_4({}^m8)8(6)^{1/2}\\
&+A_6({}^n7)A_6({}^m8)6(14)^{1/2}-r[A_2({}^n7)A_4({}^m8)5(11)^{1/2}-A_2({}^n7)A_0({}^m8)6(7)^{1/2}+A_4({}^n7)A_6({}^m8)(273)^{1/2}\\
&-A_6({}^n7)A_4({}^m8)(13)^{1/2}-A_4({}^n7)A_2({}^m8)(55)^{1/2}+A_6({}^n7)A_8({}^m8)2(35)^{1/2}]\}^2.
\end{aligned}$$